Impact of RF Front-end Nonlinearity on WSN Communications

Amine Didioui[1,2], Carolynn Bernier[1], Dominique Morche[1], and Olivier Sentieys[2]
[1]CEA/LETI - Minatec, Grenoble, France
[2]IRISA/INRIA - University of Rennes 1, Lannion, France

***Abstract*—In this paper, we study the impact of RF-front end nonlinearity on the performance of wireless sensor networks (WSN). More specifically, we investigate the problem of interference caused by intermodulation between in-band interferers. We analyze this problem using an enhanced model of signal-to-interference-and-noise ratio (SINR) that includes an interference term due to intermodulation. Using a WSN simulator and the selectivity and the third-order input intercept point (IIP_3) specifications of a radio transceiver, we show that the new SINR model provides helpful information for the analysis of intermodulation problems caused by in-band signals in IEEE 802.15.4 WSNs.**

***Index Terms*—Nonlinearity, intermodulation, RF front-end, wireless sensor networks, SINR, WSNet.**

I. Introduction

A wireless sensor network is composed of a large number of tiny and energy autonomous sensor nodes which are densely distributed over a region. Each node is equipped with a sensing device, a wireless radio transceiver, a microcontroller and a power source (battery and/or energy harvesting unit). A typical application of WSN is to collect data in domains such as environmental monitoring, urban safety, traffic monitoring and surveillance of hostile and inaccessible areas.

In this context, the IEEE 802.15.4 standard [1], with its characteristics of low complexity, low-cost and low power, fits the requirements of WSN, where energy consumption and network lifetime are primary concerns. The PHY layer specification defines operations in several bands, the most attractive for its world-wide availability being the 2.45 GHz unlicensed industrial, scientific and medical (ISM) band. In this band, 16 channels are defined for a data rate of 250 Kbit/s and a range of up to 30 m [1].

To boost the accuracy of collected data in a particular region or to develop new sensing applications, the density of deployed WSNs will inevitably be increased leading to mutual interference between adjacent networks. Furthermore, even if collisions within a wireless network can be avoided using an allocation algorithm, such as CSMA/CA with beacon mode proposed by IEEE 802.15.4 where guaranteed time slots (GTS) are allocated to each node by the network coordinator, interference from neighboring networks can never be totally avoided. In Fig.1 the coordinator of network 1 typically has no information about the active time periods of the nearby networks 2 and 3, whether these are also IEEE 802.15.4 networks or other 2.45 GHz ISM band wireless networks, such as IEEE 802.11 (Wifi) or IEEE 802.15.1 (Bluetooth).

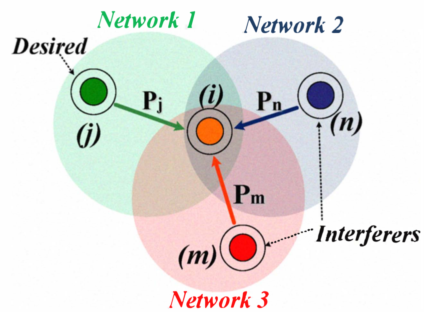

Fig. 1. Interference between desired user and nodes of adjacent networks.

Interference can lead to packet data loss, missed alarms, delay, loss of synchronization, etc. In the literature, several authors have investigated the impact of interference on WSNs using experimentation and software simulation. However, none of the existing research has studied the problem of interference due to intermodulation which is caused by the nonlinearity of the RF receiver.

This paper proposes a new SINR model for the investigating of the origin of performance degradation of WSNs under intermodulation interference. An example of how to use the new model and results from simulation, validating the model, are also presented. The network simulation is run using WSNet [2], a precise wireless sensor simulator, and is based on the parameters of a commercial IEEE 802.15.4 compliant RF transceiver.

II. State of the art SINR models

Interference in WSN has been investigated extensively in the research literature using several models. The choice of the interference model is of fundamental importance. Not only has the proposed model to implement the nature of real communications, but also to facilitate the development of rigorous analysis. One model widely used in literature [3] [4] [5] is the *standard* SINR (or short, SINR^s)

$$\mathrm{SINR}^s = \frac{P_{\text{signal}}}{N + P_{\text{interference}}} \tag{1}$$

where P_{signal} and N are respectively the desired signal and thermal noise power at the receiver front-end, while $P_{\text{interference}}$ is interference power due to the other IEEE 802.15.4 networks or types of networks operating in the same band (e.g. IEEE 802.15.1, IEEE 802.11, etc).

In practice, signal reception often takes place in the presence of different types of interference, the most commonly studied being co-channel and adjacent channel interference. An *enhanced* SINR (or short, SINR^e) model that takes into account these two types of interference was defined in [6]. The SINR^e is calculated for node i when receiving the desired signal emitted by node j and while other nodes (denoted k) are simultaneously emitting a signal (Fig. 1). The SINR^e is given by :

$$\text{SINR}^e_{i,j} = \frac{P_j}{N_i + \sum_{k \neq i,j} \alpha_{i,k} \cdot P_k} \tag{2}$$

where P_k is the power of the k^{th} interferer signal and $\alpha_{i,k}$ is a rejection factor that emulates the channel selectivity of node i and is therefore a function of the frequency offset between the RF channels occupied by node i and k. All signal powers are referred to the antenna of node i. The received signal power P_j and P_k are calculated using an appropriate channel model for the application scenario. This may be a simple pathloss model or a more elaborate statistical model to take into account fading and shadowing effects in a mobile scenario. The results of simulation using the model SINR^e are reported to be in good agreement with real-world experiments [7].

However, none of these models consider the possibility that the inherent nonlinearity of the receiver (Fig.2) can create intermodulation interference which may also corrupt the desired signal.

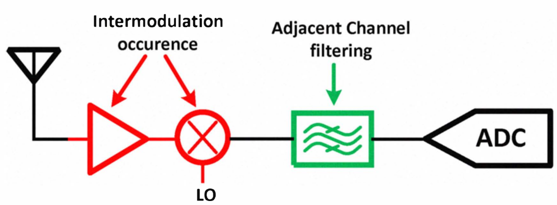

Fig. 2. Block diagram of a simple receiver.

In fact, the intermodulation interference can be observed only using an appropriate RF simulation. For this purpose, the emphasis is placed upon integration of intermodulation in WSNs simulation by extending the SINR model of (2).

III. Analysis of Intermodulation Interference

We now proceed to the study of intermodulation interference using a new, more elaborate definition of SINR.

A. Intermodulation Modeling

Intermodulation products are produced when two or more in-band signals are applied to the input of a nonlinear receiver. To analyze intermodulation, we consider the case of a memoryless nonlinear circuit which is described by the transfer function given in (3). Because the higher order products are of less significance, the transfer function order is limited to 3 in this discussion.

$$y(t) = \sum_{n=1}^{3} k_n x(t)^n \tag{3}$$

where k_n describe the coefficients of the different orders of nonlinearity, and $x(t)$ is the input signal, which is assumed to consist of two sinusoids of different frequencies such as

$$x(t) = A_1 \cos(2\pi f_1 t) + A_2 \cos(2\pi f_2 t). \tag{4}$$

Amplitudes and corresponding frequencies of the components of the output signal $y(t)$ are summarized in Table I.

TABLE I
Intermodulation Products and Their Amplitudes

Order	Frequency	Component Amplitude
1^{st} order	f_1	$k_1A_1 + \frac{3}{4}k_3A_1^3 + \frac{3}{2}k_3A_1A_2^2$
	f_2	$k_1A_2 + \frac{3}{4}k_3A_2^3 + \frac{3}{2}k_3A_2A_1^2$
2^{nd} order	$f_1 \pm f_2$	$k_2A_1A_2$
3^{rd} order	$2f_1 \pm f_2$	$\frac{3}{4}k_3A_1^2A_2$
	$2f_2 \pm f_1$	$\frac{3}{4}k_3A_1A_2^2$

As shown in Table I, the output signal $y(t)$ contains second-order intermodulation components at the sum and difference of the two frequencies f_1 and f_2. These will be neglected in the following since they either fall out of the receiver passband or, for the product at frequency $f_1 - f_2$ which falls close to direct-current (DC), are an issue for certain types of Zero-IF or Low-IF receivers only [8]. In this paper, we consider only the terms at frequencies $2f_1 - f_2$ and $2f_2 - f_1$ which are commonly referred to as third-order intermodulation distortion (IMD_3) products. As depicted in Fig. 3, if the distance between the frequencies of two in-band interferers (f_1 and f_2) is similar to the distance between one of the interferers and the useful signal at f_0, one of the resulting intermodulation products may fall close or within the receiver channel and may corrupt the desired signal.

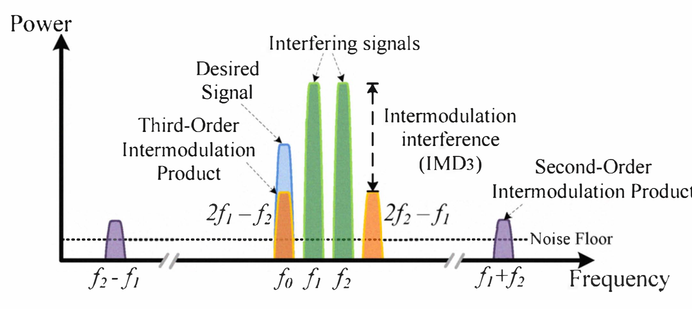

Fig. 3. Power spectrum of intermodulation product.

Using Table I, the IMD_3 is given

$$\text{IMD}_3\ [mW] = \frac{3}{4} k_3 A^3\ ;\ A = A_1 = A_2. \tag{5}$$

Next, we analyze the relationship between the third-order input intercept point IIP_3 and IMD_3. IIP_3 is a commonly used metric for defining the linearity of an RF receiver and it corresponds to the input-referred interferer power which generates intermodulation products of equal strength as the linear components. The IIP_3 is given by [8]

$$\mathrm{IIP}_3\ [dB] = \frac{1}{2}(3A - \mathrm{IMD}_3) \tag{6}$$

$$-2 \cdot \mathrm{IIP}_3\ [dB] = 10 \log \left(\frac{3}{4} k_3\right) \tag{7}$$

Using (6) and (7), we derive a new formulation of IMD_3 such as

$$\mathrm{IMD}_3\ [mW] = 10^{(-2\mathrm{IIP}_3/10)} \cdot A^3 \tag{8}$$

In practise, if $A_1 \neq A_2$, it is necessary to define two IMD_3 products

$$\mathrm{IMD}_3(f) = \begin{cases} 10^{(-2\mathrm{IIP}_3/10)} \cdot A_1^2 A_2\ ; & f = 2f_1 - f_2 \\ 10^{(-2\mathrm{IIP}_3/10)} \cdot A_1 A_2^2\ ; & f = 2f_2 - f_1 \end{cases} \tag{9}$$

Since the IIP_3 value for a given RF receiver is often published on its datasheet, Eq. (9) can be used to find the magnitude of the IMD_3 products for the interferer powers A_1 and A_2. To avoid the interference caused by third-order distortion, the receiver usually needs a very high IIP_3. However, for an RF receiver, there is generally a link between higher IIP_3 and increased power consumption.

B. Enhanced SINR model

As shown in Fig.3, intermodulation products create unwanted components at frequencies which may interfere with the desired signal. In a worst case, the IMD_3 product will fall directly into the desired channel, a phenomenon similar to co-channel interference. As the frequency offset between the IMD_3 product and the desired signal increases, their contribution to SINR degradation becomes less harmful (in a similar manner as a adjacent channel interference).

A model for SINR between nodes i and j including the distortion due to 3^{rd} order intermodulation can therefore be derived as

$$\mathrm{SINR}_{ij} = \frac{P_j}{N_i + \sum\limits_{k \neq i,j} \alpha_{i,k} \cdot P_k + P_{\mathrm{IMD}_3}} \tag{10}$$

P_{IMD_3} represents the power of interferences caused by third-order distortion products and is expressed as

$$P_{\mathrm{IMD}_3} = \sum_{k \neq l,j} \sum_{l \neq k,j} \beta_{i_{(k,l)}} \cdot P_k P_l^2 \tag{11}$$

where $\beta_{i_{(k,l)}}$, similarly to $\alpha_{i,j}$ above, is a rejection factor that varies with the frequency offset between the desired signal channel and the resulting third-order intermodulation product at frequency $2f_k \pm f_l$. The sum extends to all interference components resulting from the intermodulation of each couple of interferers.

In order to evaluate the impact of the IMD_3 products, in the following, we will assume that the IMD_3 products that fall within the desired receiver channel are treated as co-channel interference while the ones that fall out of the desired channel are treated as adjacent interference. In an RF receiver, this assumption implies that all of the intermodulation products are created before any channel filtering is applied and that the channel filtering operation is perfectly linear. Thus, the intermodulation rejection factor $\beta_{i_{(k,l)}}$ can be expressed as a function of receiver IIP_3 and $\alpha_{i,j}$ such as

$$\beta_{i_{(k,l)}}\ [mW] = \alpha_{i,2k-l} \cdot 10^{(-2\mathrm{IIP}_3/10)}. \tag{12}$$

Finally, the new SINR model (or short $\mathrm{SINR}^{\mathrm{IMD}}$) including the effect of interference intermodulation is given by

$$\mathrm{SINR}_{ij}^{\mathrm{IMD}} = \frac{P_j}{N_i + \sum\limits_{k \neq i,j} \alpha_{i,k} \cdot P_k + \sum\limits_{k \neq l,j} \sum\limits_{l \neq k,j} \beta_{i_{(k,l)}} \cdot P_k P_l^2} \tag{13}$$

The implementation of $\mathrm{SINR}^{\mathrm{IMD}}$ model in a network simulator requires the knowledge, at a given time, of all the signals concurrently received by a given node. In this work, the network simulations are run using the wireless sensor simulator WSNet [2], thanks to its support of adjacent channel interference, WSNet required only minor modifications to implement the $\mathrm{SINR}^{\mathrm{IMD}}$. In fact, intermodulation calculation, reduces the simulation speed only by 6% for 3 channels to 20% for 16 channels.

Note that none of WSN simulators reported in the literature (such as OMNet++, NS-3, etc.) supports intermodulation interference calculation few allowing even the calculation of adjacent channel interference.

IV. Simulation results using new SINR model

A. Impact of Intermodulation on BER

The 2.4 GHz PHY layer of IEEE 802.15.4 adopts the offset quadrature phase-shift keying (O-QPSK) modulation. In an additive white Gaussian noise (AWGN) channel, the bit error rate (BER) can be expressed by [9]

$$\mathrm{BER} = Q\left(\sqrt{2 \cdot \mathrm{SINR}}\right) \tag{14}$$

where $Q(x)$ is the Gaussian Q-function distribution

$$Q(x) = \frac{1}{\sqrt{2\pi}} \int_x^{+\infty} \exp\left(-\frac{u^2}{2}\right). \tag{15}$$

To evaluate the impact of the intermodulation distortion, we plot BER curves obtained using the proposed $\mathrm{SINR}^{\mathrm{IMD}}$ model with that obtained with the $\mathrm{SINR}^{\mathrm{e}}$. The simulation scenario is shown in Fig. 1. In this figure the source node j emits a 32 Bytes/s Constant Bit Rate (CBR) broadcast traffic through channel 1 of IEEE 802.15.4 2.4 GHz radio. Then, two strong interferers (m using channel 2 and n using channel 3) start jamming the network (1). The received powers at the receiver (i) from emitter (j) and interferers (m and n) are respectively $-73\ dBm$ and $-45\ dBm$.

The rejection factor $\alpha_{i,k}$ chosen for this simulation is based on interference selectivity of TI $CC2520$ [10], which is given as

$$\alpha_{i,k}[dB] = \begin{cases} 0\ ; & i = k \\ -49\ ; & 0 \leqslant i - k \leqslant 1 \\ -54\ ; & 1 < i - k \leqslant 2 \\ -55\ ; & i - k > 2 \end{cases} \tag{16}$$

IMD$_3$ power resulting form the mixing of received signals is for $i=1$, $m=2$ and $n=3$

$$\begin{aligned} P_{\mathrm{IMD}_3} = {} & \beta_{1_{(1,2)}} P_1 P_2^2 + \beta_{1_{(2,1)}} P_2 P_1^2 \\ & + \beta_{1_{(1,3)}} P_1 P_3^2 + \beta_{1_{(3,1)}} P_3 P_1^2 \\ & + \beta_{1_{(2,3)}} P_2 P_3^2 + \beta_{1_{(3,2)}} P_3 P_2^2 \end{aligned} \tag{17}$$

The IIP$_3$ of the radio chip CC2520 is $-24\ dBm$. From (17), the calculated P_{IMD_3} is $-87\ dBm$.

The simulation results are illustrated in Fig. 4. We observe that the curve obtained with the SINR^e is very close to that of SNR, which implies that the interferers in adjacent channels are highly rejected. However, the curve obtained with the new model clearly shows that the intermodulation interference impacts the BER performance and is not negligible.

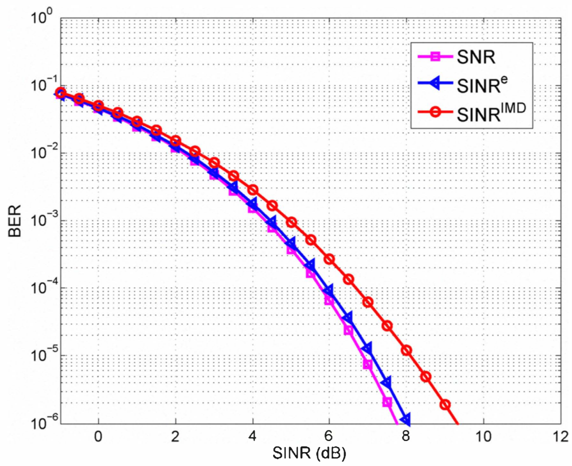

Fig. 4. Comparison of BER using different SINR models.

B. Intermodulation impact on PER

In order to further investigate the impact of intermodulation interference, another set of simulations was run using WSNet to determine the relation between PER and different channel intermodulation. In these simulations, the positions of the transmitter and the receiver were fixed, 30 m apart, and the jamming nodes were randomly distributed in a circular area around the receiver. The maximum distance between the jamming nodes and the receiver was 10 m. The simulation scenario is represented in Fig. 5.

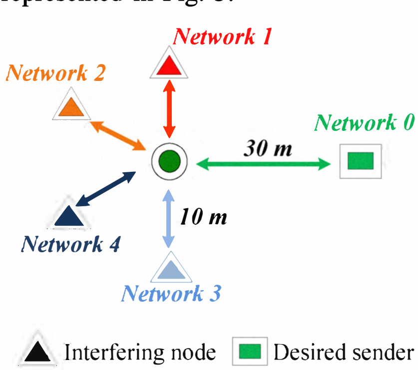

Fig. 5. Simulation scenario used for analysis of PER under intermodulation.

We consider that the power of interfering nodes exceeds the power of desired signal. Thus, the transmission power of the desired node is $-10\ dBm$, while the transmission power of the interfering nodes is 0 dBm. The received signal at the distance d from the transmitter can simply be modeled as [11]

$$P_j = P_j(d_0)\left(\frac{d}{d_0}\right)^{-n} \quad ; \quad d > d_0 \tag{18}$$

where d_0 is the reference distance and n is the path loss exponent. In this simulation, the networks use a predefined channel and adopt a non-slotted CSMA/CA and IEEE 802.15.4 2.4 GHz compliant radio. The simulation parameters are described in Table II.

TABLE II
SIMULATION PARAMETERS

Network number	channel
0	2425 MHz
1	2415 MHz
2	2420 MHz
3	2430 MHz
4	2435 MHz

Simulations are run for both SINR models, with and without intermodulation. The results obtained in terms of PER are shown in Figure 6, upon varying the node population density per jamming network, in the range 0 through 22. The diagram clearly shows the drastic impact of intermodulation on PER as the density of nodes per adjacent network increases.

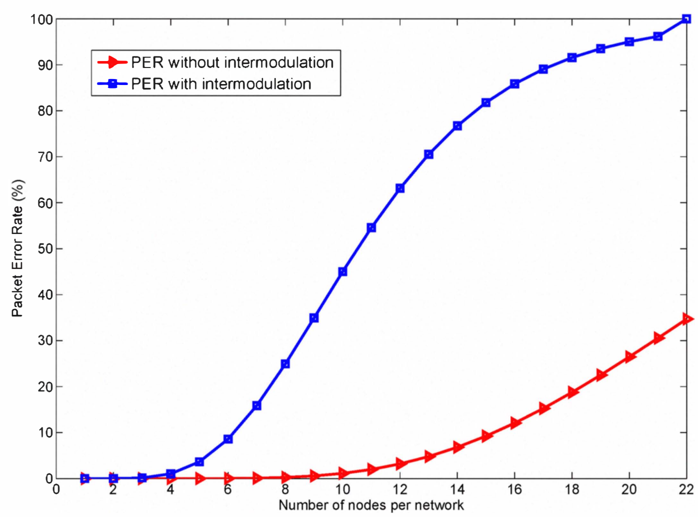

Fig. 6. Effects of node density on PER with and without intermodulation.

V. Impact of IIP$_3$ on Power Consumption and BER

Intermodulation in an RF transceiver mainly comes from the non-linearity characteristic of the different blocks in the reception chain. The linearity performance therefore depends on the circuit topology and technology. As shown in section III-A, the receiver IIP$_3$ must be sufficiently high to prevent

IMD$_3$ from degrading the SINR. However, in reality it is difficult for an active device, amplifier or mixer, especially in a very low power consumption mode to simultaneously obtain high IIP$_3$ and low noise figure (NF). Fig. 7 shows the relation between IIP$_3$ and power consumption in recently published LNAs (Low-Noise Amplifiers). The IIP$_3$ shows

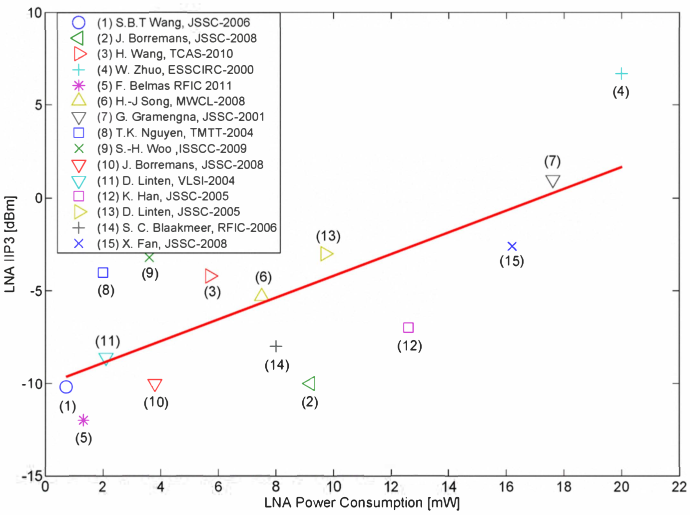

Fig. 7. IIP3 versus power consumption in recently published LNA.

a tendency to increase as power consumption increases. A simple way of avoiding intermodulation interference under low power consumption is to prevent IMD$_3$ from occurring at the receiver front-end prior to mixing. The proposed approach is to reduce the power consumption of the amplifying element prior to mixing if interference level in node environment is low. The natural candidate for gain switching is LNA, which is the first amplifier in the receiver front-end.

To assess the impact of IIP$_3$ variation on BER, we reproduce the simulation scenario of section IV-A, for multiple values of IIP$_3$: $-28\ dBm$, $-26\ dBm$, $-24\ dBm$ and $-22\ dBm$. The results are shown in Fig. 8. The solid line represents values for an interference of $-50\ dBm$ while dotted lines represent values for an interference of $-45\ dBm$.

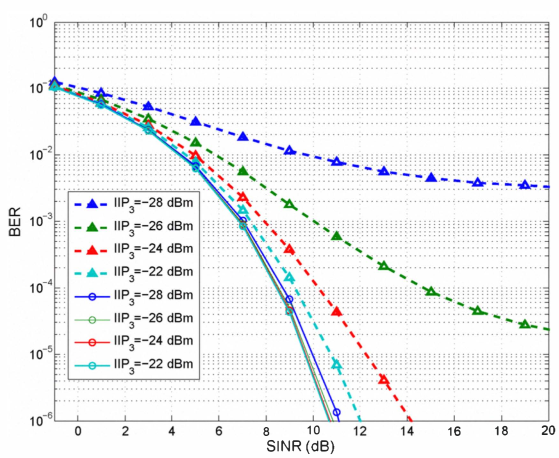

Fig. 8. Impact of IIP3 and interference power on BER.

At interference power of $-45\ dBm$, as the IIP$_3$ decreases the receiver BER also decreases due to the high magnitude of IMD$_3$. By switching interference power to $-50\ dBm$, we observe that decreasing receiver IIP$_3$ has no impact on the BER because IMD$_3$ level remains too low. Quite obviously, reducing receiver IIP$_3$ when interference power is low may considerably decrease power consumption of the node and enhance network lifetime.

VI. Conclusion

In this paper, we have thoroughly examined the IEEE 802.15.4 performance under intermodulation interference. A new model of SINR has been introduced, followed by a corresponding simulation under WSNet using parameters of IEEE 802.15.4 compliant CC2520 radio from TI. The simulation results show that intermodulation affects both BER and PER performance. If IIP$_3$ is increased, the linearity and power consumption are increased as well. Thus, in designing and deployment of WSNs particular attention should be paid to the transceiver IIP$_3$.

Acknowledgments

This work was supported by the French Armaments Procurement Agency (DGA) and the French National Research Agency (ANR) project GRECO bearing reference ANR-10-SEGI-004.

References

[1] *IEEE 802.15.4 : Wireless Medium Access Control (MAC) and Physical Layer (PHY) Specifications for Low-Rate Wireless Personal Area Networks (LR-WPANs)*, IEEE Std., 2006.

[2] G. Chelius, A. Fraboulet, and E. Benhamida, *WSNet - an Event-Driven Simulator for Wireless Networks*, http://wsnet.gforge.inria.fr/, 2008.

[3] D. G. Yoon, S. Y. Shin, W. H. Kwon, and H. S. Park, "Packet error rate analysis of ieee 802.11b under ieee 802.15.4 interference," pp. 1186–1190, 2006, vehicular Technology Conference, 2006. VTC 2006-Spring. IEEE 63rd.

[4] L. Angrisani, M. Bertocco, G. Gamba, and A. Sona, "Modeling the performance of csma-ca based wireless networks versus interference level," in *Proc. IEEE Instrumentation and Measurement Technology IMTC 2008*, 2008, pp. 376–381.

[5] A. V. Kini, N. Singhal, and S. Weber, "Performance of a wsn in the presence of channel variations and interference," in *Proc. IEEE Wireless Communications and Networking Conf. WCNC 2008*, 2008, pp. 2899–2904.

[6] E. Ben Hamida, G. Chelius, and J.-M. Gorce, "Scalable versus accurate physical layer modeling in wireless network simulations," in *Proc. 22nd Workshop Principles of Advanced and Distributed Simulation PADS '08*, 2008, pp. 127–134.

[7] H. Huo, Y. Xu, C. C. Bilen, and H. Zhang, "Coexistence issues of 2.4ghz sensor networks with other rf devices at home," pp. 200–205, 2009, sensor Technologies and Applications, 2009. SENSORCOMM '09. Third International Conference on.

[8] Q. Gu, *RF System Design of Transceivers for Wireless Communications*. Springer, 2005.

[9] J. Proakis, *Digital Communications*. McGraw Hill, 2000.

[10] TI, *CC2520 Datasheet 2.4GHz IEEE 802.15.4/ZigBee RF Transceiver*, Texas Instruments, december 2007. [Online]. Available: http://www.ti.com/lit/ds/symlink/cc2520.pdf

[11] T. S. Rappaport, *Wireless Communications: Principles and Practice*, P. H. PTR, Ed., 1996.